

GT2023-102767

THE ROLE OF TURBULENCE TRANSPORT IN MECHANICAL ENERGY BUDGETS

Pawel J. Przytarski

University of Melbourne
Melbourne, Australia

Email: pawel.przytarski@unimelb.edu.au

Davide Lengani

University of Genova
Genova, Italy

Daniele Simoni

University of Genova
Genova, Italy

Andrew P. S. Wheeler

Cambridge University
Cambridge, UK

ABSTRACT

In this paper we study the role of turbulence transport on loss prediction using high fidelity scale-resolving simulations. For this purpose we use eight high-fidelity simulation datasets and compute flux of entropy and stagnation pressure transport equation budgets for all the cases. We find that under certain unsteady inflow conditions the stagnation pressure coefficient is not a reliable loss metric even at low Mach number conditions. This is due to the turbulence transport terms. The impact of these terms, typically assumed to be negligible, made stagnation pressure loss coefficient under-predict loss from 0% to over 40% when compared to entropy loss coefficient for cases considered here. This effect was most pronounced for the cases with highly unsteady inflow conditions and at low Reynolds numbers.

NOMENCLATURE

g_{ax}	Axial gap
C_{ax}	Axial chord
h	Enthalpy
s	Entropy
ts_T	Entropy generation rate
$f.sp.$	Flux of stagnation pressure
q	Heat transfer
Ma	Mach number
\dot{m}	Mass flow rate

Pu	Periodic intensity
Tu	Turbulence intensity
p	Pressure
T	Temperature
F_{red}	Reduced frequency
Re	Reynolds number based on inlet cond. and axial chord
u	Velocity
$RANS$	Reynolds-Averaged Navier-Stokes
TKE	Turbulent Kinetic Energy
LHS	Left hand side
RHS	Right hand side
x	quantity x
X	Volume integral of x
\bar{x}	Time-average of x
x'	Fluctuating component of x
x_i	Component of a vector quantity
X_{tot}	Quantity integrated over the entire domain
X_{blw}	Quantity integrated over the boundary layer and wake regions
X_{free}	Quantity integrated over the freestream region
x^h	Related to enthalpy
x^s	Related to entropy
x^p	Related to pressure
x_t	Related to stagnation quantity
x_m	Related to mean flowfield

x_f	Related to fluctuating flowfield
x_{mf}	Related to the action of both mean and fluctuating flowfields
x_{ff}	Related to the action of fluctuating flowfield on itself

GREEK LETTERS

ρ	Density
ω	Loss coefficient
τ	Shear stress
Δ_n^+	Viscous wall units in wall-normal dir.
Δ_t^+	Viscous wall units in streamwise dir.
Δ_z^+	Viscous wall units in spanwise dir.
ϕ	Viscous dissipation
Φ	Integrated viscous dissipation
ε	Artificial dissipation
\mathcal{T}	Energy transfer between flowfields (turbulence production)
Ω	Volume of a domain

INTRODUCTION

High fidelity simulations provide the details of the entire flow field in the blade passage and therefore may be used to explore loss generation and loss generating mechanisms [1]. The most commonly used loss metric is the the stagnation pressure loss coefficient. This is because it can be directly measured and is a workhorse for evaluating the performance of different blade designs experimentally. There are other available metrics, such as entropy [2] or mechanical work potential [3], which have an advantage of better representing the lost work due to their ability to account for heat transfer and thermal mixing effects. However, they rely on quantities which are difficult to measure or have to be derived (e.g. entropy cannot be measured directly). As a result they are difficult to implement experimentally and lead to high levels of measurement uncertainty. It is therefore of interest to investigate complete transport equations using high fidelity simulations and compare loss drivers between different loss metrics.

Transport equations have been practically used since the 80s. Among the first, the work of Moore et al. [4] used mean part of the Reynolds decomposed transport equation of stagnation pressure (e.g., [5]) and applied it to the 2D-field measurements performed by means of hot-wire probes. They found that the integration of the production of the turbulence kinetic energy represented the generation of stagnation pressure loss well. Similarly, more recent papers, either experimental (e.g., [6–8]) or numerical (e.g., [9, 10]) made strides to understand the mechanism by which turbulence extracts work from the mean flow via turbulence production. The interest in the production of turbulence kinetic energy is partially motivated by the relative ease of computing it from the experimental data with relatively low uncertainty. On the other hand, other terms appearing in the trans-

port equations are difficult to obtain and are often neglected. For this reason, the transport equation of entropy, that relates the entropy generation rate to the viscous dissipation and heat transfer terms has been computed in more recent high-fidelity simulations (e.g., [11–16]). These authors showed that the full volume integration of the right hand side of the entropy transport equation may provide a spatial breakdown of losses pointing out at their sources. In addition, Leggett et al. [15] provided a comparison of entropy and mechanical work potential terms appearing in the respective transport equations.

In the present paper we will compare different loss coefficients computed from several unsteady high-fidelity simulations of compressor blades and we will further discuss the results computing the full transport equation of entropy and stagnation pressure flux. The paper is structured as follow: (1) the global loss coefficients are introduced; (2) The numerical methods and simulation cases are summarised; (3) transport equations of entropy flux and stagnation pressure flux are analysed to provide a rationale for a comparison of the metrics; (4) the result section that discusses the different loss coefficients and loss budgets with a focus on the effect of turbulence on the different budgets.

In particular, the paper will address the following questions:

1. How do loss coefficients vary for the considered cases?
2. What determines the loss coefficients of interest?
3. What is the role of turbulence transport in loss prediction?

COMPUTATIONAL SETUP

Solver details

For this study we use high-fidelity datasets of Przytarski and Wheeler [12, 14]. These datasets were generated using the high-order compressible Navier–Stokes solver *3DNS* [17]. In total, eight datasets were used which consisted of two *NACA65* datasets at steady turbulent inflow conditions, three *NACA65* datasets at unsteady inflow conditions akin to multi-stage environment and three *CDA* (Controlled Diffusion Airfoil) datasets unsteady inflow conditions akin to multi-stage environment. Table 1 summarises the datasets and shows the running conditions of each case. For cases with unsteady inflow conditions reduced frequency F_{red} was also reported and the unsteadiness intensity was decomposed into periodic Pu and turbulent Tu components. The spanwise extent for *NACA65* cases was 10% of the axial chord, while *CDA* cases used spanwise extent equal to 15% of axial chord. Maximum viscous wall for these geometries are reported in Table 2 asserting the wall-resolved accuracy. Setup details and a more thorough description of each case, including a procedure used to mimic the multi-stage environment, can be found in [12, 14]. An example of an instantaneous flowfield for steady and unsteady *NACA65* profile as well as an unsteady *CDA* profile can be seen in Figure 1 for which the spanwise vorticity contours were plotted.

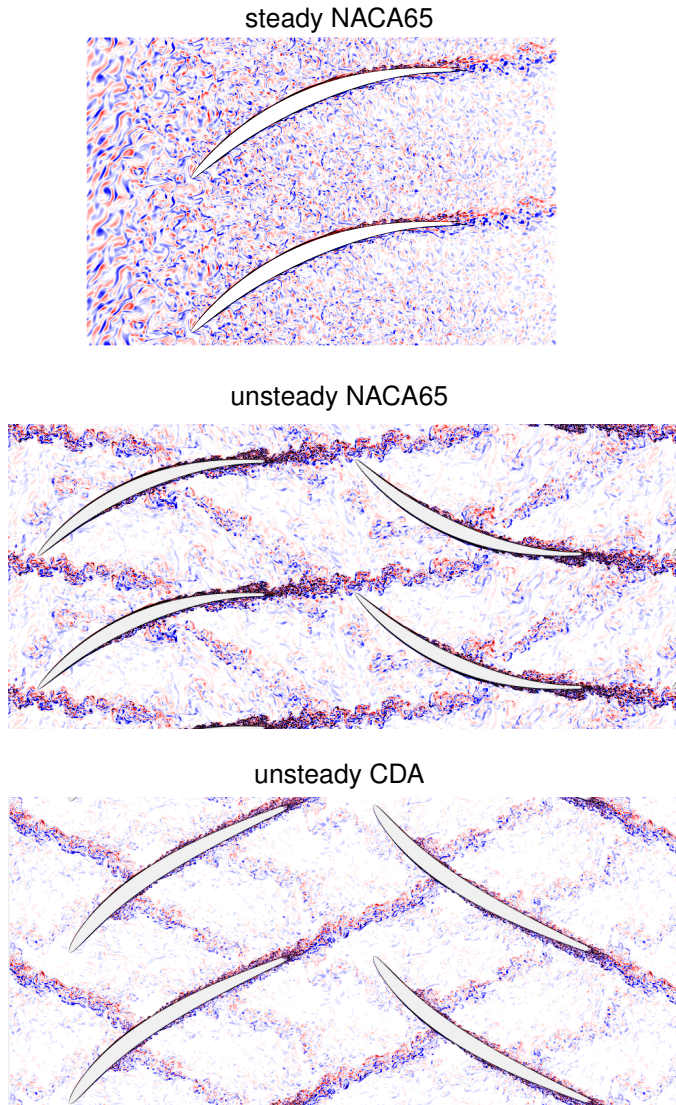


FIGURE 1: Instantaneous spanwise vorticity flowfield for 3 example cases considered here: *NACA65 – Tu4* (top), *NACA65 – Gap40* (center) and *CDA – Gap40* (bottom).

LOSS METRICS

As discussed by Denton [2], there are several loss coefficients that are used in turbomachinery. The most popular loss coefficients are entropy, enthalpy and stagnation pressure loss coefficients. As asserted by Denton [2], entropy and enthalpy loss coefficients should report virtually identical results. However, the advantage of entropy loss coefficient is that it is more applicable in the engine setting. More in-depth discussion on the limitations of each loss coefficient can be found in the literature e.g. [18, 19].

TABLE 1: Details of 2 steady and 6 unsteady inflow cases

Geometry	Case	Re	Ma	F_{red}	Pu	Tu
<i>NACA65</i>	<i>Tu4</i>	140k	0.065	–	–	4.0%
<i>NACA65</i>	<i>Tu6</i>	140k	0.065	–	–	6.0%
<i>NACA65</i>	<i>Gap30</i>	140k	0.065	1.71	5.0%	4.2%
<i>NACA65</i>	<i>Gap40</i>	140k	0.065	1.71	3.6%	3.3%
<i>NACA65</i>	<i>Gap50</i>	140k	0.065	1.71	3.0%	2.9%
<i>CDA</i>	<i>Gap30</i>	250k	0.20	2.49	4.9%	3.1%
<i>CDA</i>	<i>Gap40</i>	250k	0.20	2.49	3.7%	2.9%
<i>CDA</i>	<i>Gap50</i>	250k	0.20	2.49	3.2%	3.0%

TABLE 2: Maximum near-wall viscous units

Case	$Mesh$	Δ_n^+	Δ_t^+	Δ_z^+
steady <i>NACA65</i>	73M	0.9	7	7
unsteady <i>NACA65</i>	130M	0.6	4.8	6.0
unsteady <i>CDA</i>	170M	0.9	15.5	10.0

Despite the consensus that entropy loss coefficient is the most accurate for engine performance evaluation, the industrial practice often relies on stagnation pressure loss coefficient due to the ease of measuring it in an experimental setting. However, in our experience it is often difficult to obtain consistent results from entropy and stagnation pressure loss coefficients. Given the availability of relevant high-fidelity datasets, it is desirable to study the predictive capability of these loss coefficients, what determines them and their limitations for the unsteady, turbulent turbomachinery flows.

Entropy loss coefficient

Entropy loss coefficient can be computed from high-fidelity data directly by taking time-averaged and flux-averaged entropy at the inlet and outlet of the integration domain:

$$\omega^s = \frac{T_2(s_2 - s_1)}{h_{t,1} - h_1} \quad (1)$$

TABLE 3: The summary of loss coefficients for all the cases

Loss	NACA65		NACA65			CDA		
	Tu4	Tu6	Gap30	Gap40	Gap50	Gap30	Gap40	Gap50
ω^s	0.0290	0.0383	0.0271	0.0259	0.0262	0.0229	0.0208	0.0208
$\omega^{s(T,p)}$	0.0296	0.0390	0.0284	0.0267	0.0270	0.0234	0.0213	0.0212
ω^h	0.0296	0.0390	0.0284	0.0267	0.0270	0.0235	0.0213	0.0212
ω^p	0.0255	0.0287	0.0145	0.0186	0.0205	0.0207	0.0207	0.0206
$\omega_{no\ TKE}^p$	0.0225	0.0180	0.0067	0.0128	0.0161	0.0149	0.0151	0.0153

alternatively, entropy can be approximated with time-averaged and flux-averaged pressure and temperature:

$$s - s_{ref} = C_p \ln(T/T_{ref}) - R \ln(p/p_{ref}) \quad (2)$$

to compute the derived entropy loss coefficient:

$$\omega^{s(T,p)} = \frac{T_2(s_{(T,p)2} - s_{(T,p)1})}{h_{t,1} - h_1} \quad (3)$$

Enthalpy loss coefficient

Enthalpy loss coefficient can be computed according to:

$$\omega^h = \frac{h_2 - h_{2s}}{h_{t,1} - h_1} \quad (4)$$

and is a popular choice for the design practice as it is independent of the Mach number.

Stagnation pressure loss coefficient

The stagnation pressure loss coefficient can be obtained experimentally by directly measuring total pressure which can be time-averaged and flux-averaged:

$$\omega^p = \frac{p_{t,1} - p_{t,2}}{p_{t,1} - p_1} \quad (5)$$

This is the most commonly used loss coefficient and it is generally accepted that it is an accurate estimate, at least in the limit of low Mach numbers. When stagnation pressure is measured at

sufficiently high frequency at incompressible limit the stagnation pressure formula reads:

$$p_t = \bar{p} + \frac{1}{2} \bar{u}_i \bar{u}_i + \frac{1}{2} \overline{u'_i u'_i} \quad (6)$$

where $\frac{1}{2} \bar{u}_i \bar{u}_i$ represents mean kinetic energy and $\frac{1}{2} \overline{u'_i u'_i}$ represents turbulent kinetic energy. However, in practice, when unsteadiness is low enough, turbulent part of the kinetic energy is discarded resulting in:

$$p_{t,no\ TKE} = \bar{p} + \frac{1}{2} \bar{u}_i \bar{u}_i \quad (7)$$

Equations 6 and 7 are in practice used interchangeably, but at highly unsteady flowfields they result in different stagnation pressure estimates and may have an impact in particular when comparing experimental results against RANS derived predictions. Definition in equation 6 arise from the flux of stagnation pressure equation that will be shown later (eq. 15a), while definition in equation 7 arise from the mean kinetic energy flow equation, shown in Appendix A (eq. 20a). Both of these definitions can be used to obtain a stagnation pressure loss coefficient which will be referred to as:

$$\begin{aligned} \omega^p & \quad \text{- for stagnation pressure including TKE} \\ \omega_{no\ TKE}^p & \quad \text{- for stagnation pressure without TKE} \end{aligned}$$

In this paper we will explore the impact of turbulent kinetic energy on these predictions and the role turbulent transport plays in stagnation pressure loss coefficient in general.

EVALUATION OF LOSS COEFFICIENTS

Table 3 gives a summary of above mentioned loss coefficients for all the cases considered here. For the steady cases, i.e.

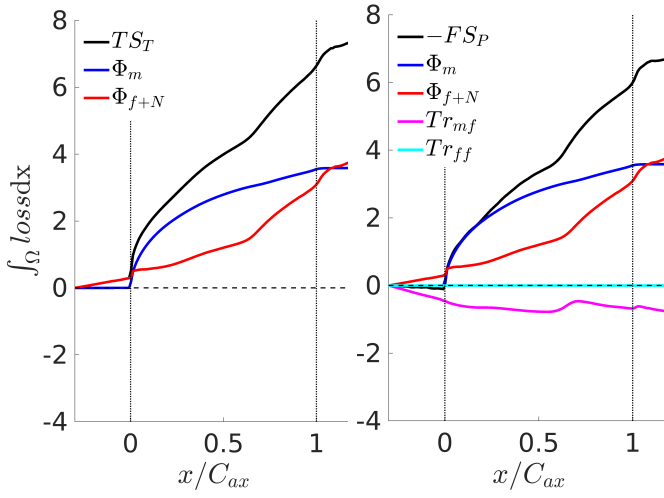


FIGURE 2: Comparison of loss contributions to entropy (left) and stagnation pressure (right) loss metrics for the steady inflow *NACA65 Tu4* case.

NACA65 Tu4 and *Tu6* the reference planes which were used to compute the loss coefficients were set at 30% axial chord upstream of the leading edge and downstream of the trailing edge. For the unsteady cases the reference planes were set at the domain inlet (20 – 40% upstream of the leading edge depending on the gap) and at the sampling plane which was located at roughly 10% axial chord downstream of the trailing edge.

As evident from the Table 3, both entropy and enthalpy loss coefficients result in closely matching estimates. On the other hand, the pressure loss coefficient (ω^p) results in values which are not only quantitatively different, but also qualitatively misleading by reversing the loss trend for unsteady *NACA65* cases. These values were highlighted in red. The estimates are even worse when stagnation pressure loss coefficient without the inclusion of turbulent kinetic energy ($\omega_{no\ TK E}^p$) is considered (also highlighted in red). This emphasises the need of including turbulent kinetic energy for stagnation pressure estimates when highly unsteady flowfields are considered.

To understand why the stagnation pressure coefficient (ω^p) is inaccurate, in the next section we will examine entropy and stagnation transport equations.

LOSS TRANSPORT EQUATIONS

The loss coefficients give us an estimate of losses in a global sense so that an overall performance of a system can be assessed. However, with all the information that high-fidelity datasets offer, these losses can be studied in more detail by examining their transport equations. Here, specifically we will consider entropy transport equation and stagnation pressure transport equation.

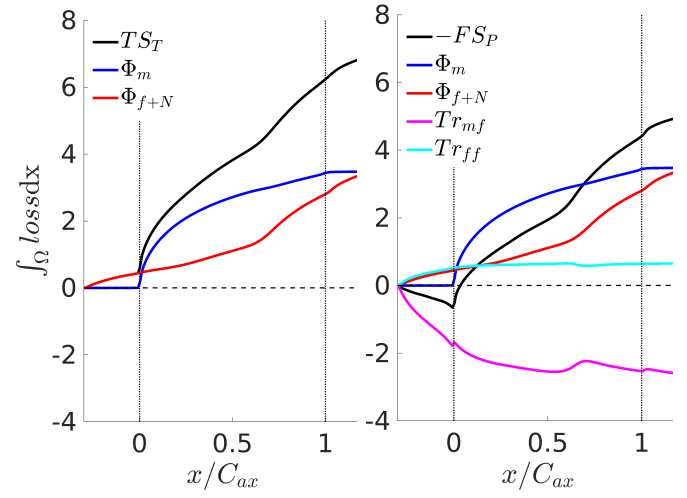


FIGURE 3: Comparison of loss contributions to entropy (left) and stagnation pressure (right) loss metrics for the unsteady inflow *NACA65 Gap40* case.

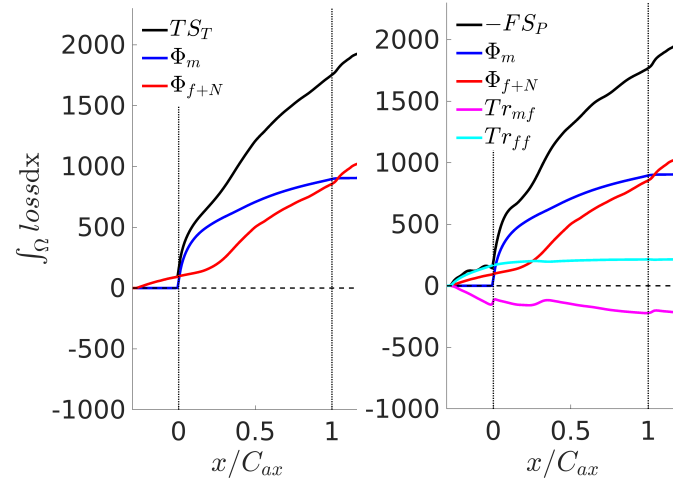


FIGURE 4: Comparison of loss contributions to entropy (left) and stagnation pressure (right) loss metrics for the unsteady inflow *CDA65 Gap40* case.

To study these transport equations all the quantities will be integrated in the volume, Ω , between the same reference planes as were used for the computations of loss coefficients. Throughout the paper the integrated quantities are capitalized, for instance the integrated dissipation will be:

$$\Phi = \int_{\Omega} \phi d\Omega \quad (8)$$

and since the simulation were compressible, all quantities used in the budgets are Favre-averaged:

$$\bar{f} \equiv \frac{\overline{\rho f}}{\bar{\rho}} \quad (9)$$

Entropy transport equation

First we examine the entropy transport equation, [20]:

$$\rho \frac{Ds}{Dt} = \left(\frac{1}{T} \tau_{ij} \frac{\partial u_i}{\partial x_j} \right) + \kappa \left(\frac{(\nabla T)^2}{T^2} \right) - \left(\nabla \cdot \frac{q}{T} \right) \quad (10)$$

To gain further insight we may decompose the flowfield into mean and turbulent components by performing Reynolds decomposition:

$$f = \bar{f} + f' \quad (11)$$

For the purpose of comparing the flux of entropy with the flux of stagnation pressure we rearrange the equation so that the left hand side is akin to $T\Delta s$ term, while the right hand side has contributions which are due to the viscous dissipation and heat transfer terms. Following a similar procedure as the one outlined in [21], we obtain:

$$\begin{aligned} \overline{T\rho \frac{Ds}{Dt}} &= \underbrace{\overline{\tau_{ij} \frac{\partial \bar{u}_i}{\partial x_j}}}_{\phi_m} + \underbrace{\overline{\tau'_{ij} \frac{\partial u'_i}{\partial x_j}}}_{\phi_f} \\ &+ \underbrace{\kappa \frac{1}{\bar{T}} \left(\frac{\partial \bar{T}}{\partial x_i} \right)^2}_{irq_m} - \underbrace{\bar{T} \frac{\partial}{\partial x_i} \left(\frac{\bar{q}_i}{\bar{T}} \right)}_{rq_m} - \underbrace{\bar{T} \frac{\partial}{\partial x_i} \left(\frac{\bar{q}'_i}{\bar{T}} \right)}_{rq_f} \end{aligned} \quad (12a)$$

where

- ts - entropy generation rate
- ϕ_m - viscous dissipation due to mean strains
- ϕ_f - turbulent viscous dissipation
- irq_m - mean flow irreversible heat transport
- rq_m - mean flow reversible heat flux
- rq_f - turbulent reversible heat flux

The first two terms on the right-hand-side are the irreversible entropy changes due to viscous friction while the terms three, four and five are the irreversible and reversible changes in entropy due to heat transfer. For the cases considered in this paper, integrated heat transfer terms are negligible (adiabatic, low Mach

numbers). It is also important to point out that in a computational sense, another term comes about, ε_N , due to the combined effects of discretization errors and numerical filtering (artificial dissipation). As a result for cases considered here the flux of entropy budgets can be computed as:

$$\underbrace{\int T\rho \frac{Ds}{Dt} d\Omega}_{TS_T} \approx \underbrace{\int \left(\overline{\tau_{ij} \frac{\partial \bar{u}_i}{\partial x_j}} \right) d\Omega}_{\Phi_m} + \underbrace{\int \left(\overline{\tau'_{ij} \frac{\partial u'_i}{\partial x_j}} + \varepsilon_N \right) d\Omega}_{\Phi_{f+N}} \quad (13)$$

Equation 13 suggests that for adiabatic flows at low Mach numbers, entropy comes about purely as a result of viscous dissipation. It also allows for the estimation of artificial dissipation term, ε_N caused by the insufficient mesh resolution. This fact was previously used by Przytarski and Wheeler [14] to assess the simulation resolution and a more in-depth discussion of entropy budgets can be found there. We further assert that the artificial dissipation can be accounted to the turbulent viscous dissipation by performing Reynolds decomposition of kinetic energy and computing full budget for both mean and turbulent components. This is shown in Appendix A. Consequently, for the remainder of the paper, we will refer to the combined resolved and unresolved turbulent viscous dissipation as Φ_{f+N} .

Stagnation pressure transport equation

To obtain the flux of stagnation pressure, momentum and continuity equations can be rearranged to obtain:

$$\frac{Dp_t}{Dt} \approx \frac{D(\rho \frac{1}{2} u_i u_i)}{Dt} + u_i \frac{\partial p}{\partial x_j} = u_i \frac{\partial \tau_{ij}}{\partial x_j} \quad (14)$$

As before, we can gain more insight by decomposing the flowfield into mean and turbulent components by performing Reynolds decomposition and averaging with respect to time as shown in ([22], p. 71):

$$\begin{aligned} \underbrace{\overline{\frac{Dp_t}{Dt}}}_{fsp} &\approx \underbrace{\frac{\bar{D}}{Dt} \left(\bar{\rho} \frac{1}{2} \bar{u}_i \bar{u}_i \right)}_{adv_m} + \underbrace{\frac{\bar{D}}{Dt} \left(\bar{\rho} \frac{1}{2} \overline{u'_i u'_i} \right)}_{adv_f} + \underbrace{\bar{u}_i \frac{\partial \bar{p}}{\partial x_j}}_{pw_m} = \\ &- \underbrace{\overline{\tau_{ij} \frac{\partial \bar{u}_i}{\partial x_j}}}_{\phi_m} - \underbrace{\overline{\tau'_{ij} \frac{\partial u'_i}{\partial x_j}}}_{\phi_f} - \underbrace{\frac{\partial}{\partial x_j} \left[\bar{u}_i \left(\overline{\rho u'_i u'_j} \right) \right]}_{tr_{mf}} - \underbrace{\frac{\partial}{\partial x_j} \left[\overline{\rho u'_j} \left(\frac{1}{2} \overline{u'_i u'_i} \right) \right]}_{tr_{ff}} \\ &+ \underbrace{\frac{\partial \bar{\tau}_{ij} \bar{u}_i}{\partial x_j}}_{vd_m} + \underbrace{\frac{\partial \overline{\tau'_{ij} u'_i}}{\partial x_j}}_{vd_f} + \underbrace{\bar{u}_i \frac{\partial \bar{p}}{\partial x_j}}_{pw_f} - \underbrace{\frac{\partial \overline{p' u'_i}}{\partial x_j}}_{pd_f} + \underbrace{\overline{p' \frac{\partial u'_i}{\partial x_j}}}_{pl_f} \end{aligned} \quad (15a)$$

TABLE 4: Flux of entropy transport equation budgets

$$TS_T \approx \Phi_m + \Phi_{f+N}$$

	NACA65		NACA65			CDA		
	Tu4	Tu6	Gap30	Gap40	Gap50	Gap30	Gap40	Gap50
TS_T	7.564	9.954	6.980	6.668	6.726	2111.269	1916.130	1916.756
Φ_m	3.588	3.660	3.419	3.472	3.554	962.015	904.669	911.772
Φ_{f+N}	3.976	6.295	3.561	3.196	3.172	1149.254	1011.461	1004.984
$\omega^s(TS_T)$	0.0295	0.0388	0.0272	0.0260	0.0263	0.0234	0.0213	0.0213
ω_m^s	0.0290	0.0383	0.0271	0.0259	0.0262	0.0229	0.0208	0.0208

where

- fsp - flux of stagnation pressure
- adv - convection of kinetic energy
- pw - pressure work
- tr - turbulent transport due to unsteadiness
- vd - viscous diffusion
- ϕ - viscous dissipation
- pd - pressure diffusion
- pl - pressure dilation



FIGURE 5: Example domain decomposition for the NACA65 Tu4 case.

LOSS TRANSPORT EQUATIONS BUDGETS AND LOSS COEFFICIENTS

Entropy and stagnation pressure transport equations can be directly related to loss coefficients:

$$\omega^s(TS_T) = \frac{T_2(s_2 - s_1)}{h_{t,1} - h_1} \approx \frac{1}{h_{t,1} - h_1} \frac{TS_T}{\dot{m}} \quad (16a)$$

$$\omega^p(FSP) = \frac{p_{t,1} - p_{t,2}}{p_{t,1} - p_1} \approx \frac{\rho_{ref}}{p_{t,1} - p_1} \frac{-FSP}{\dot{m}} \quad (16b)$$

as a result, we are now able to split each loss coefficient into its constituent components and comment directly on their relative importance:

$$TS_T = \Phi_m + (\Phi_{f+N}) \quad (17a)$$

$$-FSP = \Phi_m + (\Phi_{f+N}) \quad (17b)$$

$$+ \underbrace{Tr_{mf} + Tr_{ff} - VD_m - VD_f - PW_f + PD_f - PL_f}_{\text{typically assumed} \approx 0}$$

As mentioned before, for cases considered here, the entropy loss coefficient is driven purely by the viscous dissipation, conveniently split into dissipation due to mean strains Φ_m and turbulent dissipation Φ_{f+N} (the sum of resolved and unresolved components).

The stagnation pressure loss coefficient arise as an interplay between dissipation due to mean strains Φ_m , turbulent dissipation Φ_{f+N} , turbulent transport due to mean and turbulent fields Tr_{mf} and Tr_{ff} , mean and turbulent viscous diffusion VD_m and VD_f , as well as turbulent pressure work PW_f , pressure diffusion PD_f and pressure dilation PL_f . It should be mentioned that since

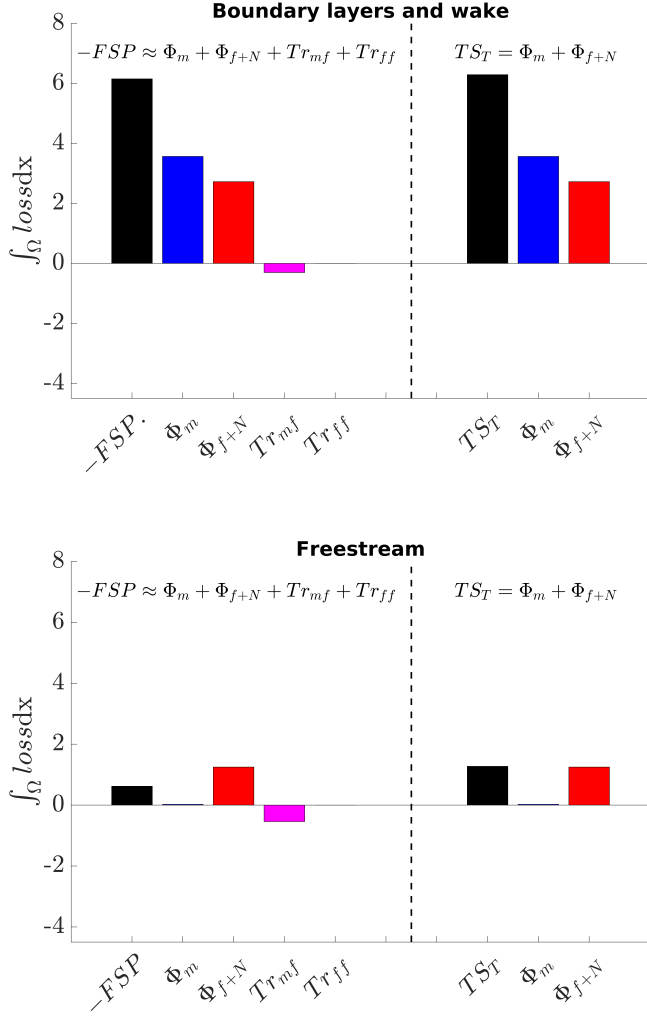


FIGURE 6: Comparison of loss contributions for the steady inflow *NACA65 Tu4* case for boundary layers and wake (top) and freestream (bottom).

Moore et al. [4], the diffusive terms ($Tr_{mf,ff}$, $VD_{m,f}$, PW_f , PD_f , PL_f) are often neglected as it is assumed that their volume integral is negligible. Furthermore, there are practical difficulties estimating these terms experimentally. High-fidelity datasets are immune to such limitations and so are perfect test bed for verifying these assumptions under a variety of conditions.

Table 4 shows the flux of entropy budgets for all the cases. Below the budget, entropy loss coefficient derived from the budget is compared to the one computed globally at the reference frames. Very good agreement is shown between these two loss coefficients.

Similarly, Table 5 shows the flux of stagnation pressure budgets for all the cases. At the bottom of the table the stagnation

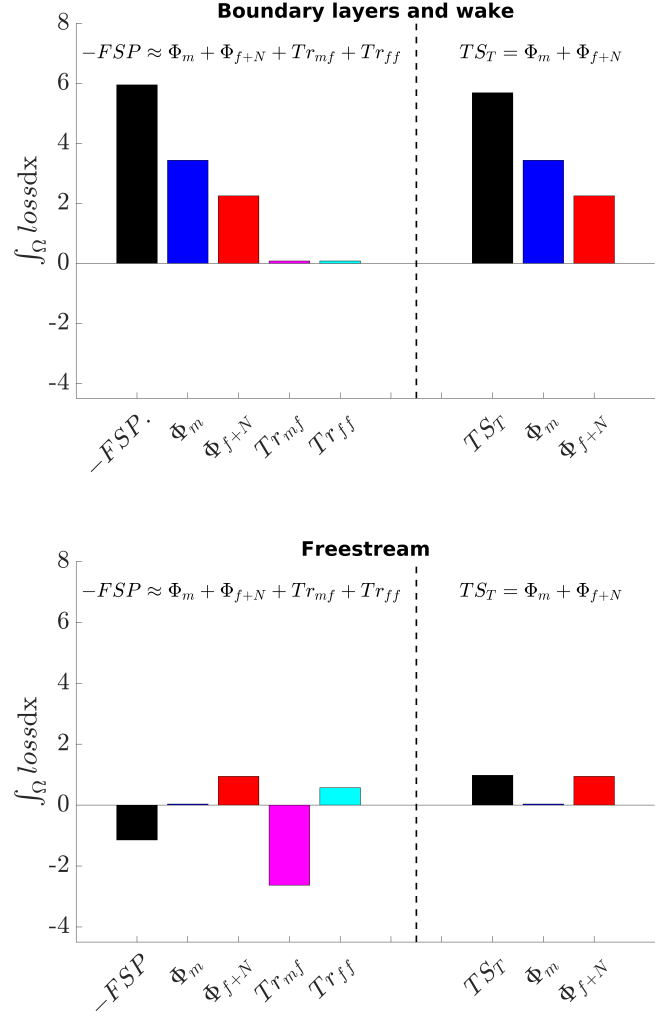


FIGURE 7: Comparison of loss contributions for the unsteady inflow *NACA65 Gap40* case for boundary layers and wake (top) and freestream (bottom)..

pressure loss coefficient derived from the budget is compared to the one computed globally and, again, a good agreement is shown between these two loss coefficients for all the cases.

Some of the terms in the flux of stagnation pressure budgets (mainly PW_f , PL_F) were not possible to compute and as a result were not considered. Despite omitting them in the budget, the difference between left hand side and the right hand side terms (LHS-RHS) is small and it is therefore concluded that these terms can be considered negligible for the cases considered here.

In the next section we will explore how the components of these loss budgets determine the overall loss coefficient.

TABLE 5: Flux of stagnation pressure transport equation budgets

$$-FSP = \Phi_m + \Phi_{f+N} + Tr_{mf} + Tr_{ff} - VD_m - VD_f - PW_f + PD_f - PL_f$$

	NACA65		NACA65			CDA		
	Tu4	Tu6	Gap30	Gap40	Gap50	Gap30	Gap40	Gap50
$-FSP$	6.771	7.656	3.819	4.810	5.317	1,860.353	1,931.734	1,972.560
$-Adv_m - Adv_f - PW_m$	6.691	7.576	3.811	4.801	5.308	1,816.369	1,891.532	1,929.971
Φ_m	3.588	3.660	3.419	3.472	3.554	962.015	904.669	911.772
Φ_{f+N}	3.976	6.295	3.561	3.196	3.172	1149.254	1011.461	1004.984
Tr_{mf}	-0.847	-2.587	-3.905	-2.551	-2.004	-387.640	-207.121	-208.588
Tr_{ff}	-	-	0.688	0.649	0.488	94.282	213.863	202.576
$-VD_m$	-0.012	-0.009	-0.014	-0.015	-0.015	-2.451	-2.229	-2.240
$-VD_f$	-0.008	-0.017	-0.005	-0.005	-0.005	-1.881	-1.577	-1.544
$-PW_f$	-	-	-	-	-	-	-	-
PD_f	-	-	0.129	0.080	0.111	4.810	26.336	33.456
$-PL_f$	-	-	-	-	-	-	-	-
LHS - RHS	-0.073	-0.315	0.054	0.016	-0.016	-41.965	13.668	-32.144
$\omega^p(FSP)$	0.0264	0.0298	0.0149	0.0187	0.0208	0.0204	0.0212	0.0217
ω_m^p	0.0255	0.0287	0.0145	0.0186	0.0205	0.0207	0.0207	0.0206

COMPARISON OF LOSS CONTRIBUTIONS

The first thing to note from Table 5 is that while most diffusive terms are indeed close to zero and negligible as typically assumed, however the turbulent transport terms Tr_{mf} and Tr_{ff} are consistently high and range from 15% of turbulence dissipation Φ_f for the moderate turbulence *NACA65 Tu4* case, all the way to over 100% for the unsteady *NACA65 Gap30* case.

This is further demonstrated by integrating all the budgets along the streamwise direction to obtain a line integral plots for the steady *NACA65 Tu4* case, Figure 2, unsteady *NACA65 Gap40* case, Figure 3 and unsteady *CDA Gap40* case, Figure 4. For all the cases the domain was normalised by the axial chord with $x = 0$ coordinate corresponding to the leading edge and $x = 1$ coordinate corresponding to the trailing edge.

Turbulent transport terms Tr_{mf} and Tr_{ff} play a significant role in stagnation pressure transport equation for most of the con-

sidered cases. For *CDA* cases their impact appears to be limited as both terms are of similar magnitude and opposite sign and therefore lead to error cancellation.

It can be also noted that turbulent transport terms have stronger impact on the cases that feature more unsteady/turbulent inflow. As a result, by the virtue of how stagnation pressure transport is computed and due to the terms' negative contribution, they reduce the stagnation pressure loss coefficient resulting in erroneous performance prediction.

To understand where the impact of turbulent transport terms is the strongest we perform a domain decomposition and compute a loss budget for different regions. We determine the boundary layer and the wake edges with a vorticity criterion. Figure 5 shows the resulting region split. Figure 6 shows separate budgets for the combined regions of boundary layers and wake and for the freestream for the steady inflow *NACA65 Tu4* case. Simi-

TABLE 6: Entropy and stagnation pressure loss prediction for the combined region of boundary layers and wake and for freestream

	NACA65		NACA65			CDA		
	Tu4	Tu6	Gap30	Gap40	Gap50	Gap30	Gap40	Gap50
$TS_{T,tot}$	7.564	9.954	6.980	6.668	6.726	2111.269	1916.130	1916.756
$-FSP_{tot}$	6.770	7.656	3.819	4.810	5.317	1860.353	1931.734	1972.560
$TS_{T,blw}$	6.289	6.616	5.836	5.688	5.789	1771.757	1610.546	1627.988
$-FSP_{blw}$	6.149	6.331	6.338	5.953	5.956	1449.368	1441.570	1424.509
$TS_{T,free}$	1.2752	3.3381	1.1441	0.9799	0.9377	339.5117	305.5845	288.7683
$-FSP_{free}$	0.622	1.325	-2.519	-1.143	-0.639	410.985	490.164	548.050
$-FSP_{blw}/TS_{T,blw}$	97.77%	95.69%	108.61%	104.66%	102.90%	96.43%	106.38%	102.90%
$-FSP_{free}/TS_{T,free}$	48.76%	39.70%	-220.16%	-116.63%	-68.17%	36.17%	64.81%	102.99%

larly, Figure 7 shows analogous budget for the unsteady inflow *NACA65 Gap40* case. The overall loss comparison for the remaining cases is given in Table 6. It is clear from both figures that vast majority of turbulent transport Tr_{mf} and Tr_{ff} happens in the freestream. As a result the loss, as predicted by stagnation pressure, is well predicted for the boundary layers and wake regions, however, it reduces in the freestream which skews the overall loss prediction. This was the case for most of the datasets considered here. For two *CDA* cases with *Gap40* and *Gap50* that effect was negligible as the two turbulent transport terms were of similar magnitude and opposite signs.

The results suggest that even for the cascades exposed to moderate levels of freestream turbulence, stagnation pressure loss coefficient may lead to incorrect predictions, especially when cases with varying or unsteady inflow conditions are considered.

To understand why turbulent transport by the mean flow Tr_{mf} is negative we can inspect the formula behind the term:

$$tr_{mf} = \frac{\partial}{\partial x_j} \left[\bar{u}_i \left(\overline{\rho u'_i u'_j} \right) \right] \quad (18)$$

In the freestream the Reynolds stress terms $\overline{\rho u'_i u'_j}$ are expected to universally decay at the steady rate. For a compressor this decay is combined with a flow deceleration (\bar{u}_i). As a result (also because of the sign of the term) the overall contribution to the

stagnation pressure budget is negative, artificially lowering the predicted loss. We argue that this situation will be reverse for the turbine cases in which rapid flow deceleration is present such that the stagnation loss coefficient will result in artificially higher values. We expect this to be the case when meaningful levels of turbulence/periodic unsteadiness (2 – 3% or above) is present. The erroneous stagnation pressure loss coefficient behaviour happens irrespective of low Mach number conditions and is purely related to the freestream unsteadiness and turbulence transport term that arise due to it.

To understand why turbulent transport by the turbulent flow Tr_{ff} is positive for the unsteady inflow cases considered here we can inspect the formula behind the term:

$$tr_{ff} = \frac{\partial}{\partial x_j} \left[\overline{\rho u'_j \left(\frac{1}{2} u'_i u'_i \right)} \right] \quad (19)$$

The unsteady inflow cases consisted of periodic wakes which have an appearance of u' , v' fluctuations. These fluctuations grow in size as the wake is initially accelerated and turned when entering the passage and subsequently diffused in the aft portion of it. Such behaviour would result first in an increase of Tr_{ff} term and then its slow reduction. Figures 3 and 4 suggest that the initial acceleration and turning dominate and determine the magnitude of this term which then stays relatively constant for the remain-

der of the passage where it is diffused.

We can also determine which components of the turbulent transport contribute the most. This is shown in Table 7 which demonstrates that for the cases considered here two terms associated with the $u'u'$ and $u'v'$ Reynolds stresses are responsible for the entire turbulent transport Tr_{mf} (other terms were close to 0). This is encouraging as it suggests that at a mid-span section the turbulent transport term can be successfully estimated experimentally by considering only these two components alone and measuring Reynolds stress components associated with them. This has been demonstrated before by Perdichizzi et al [23] or Jelly et al. [24]. The role of turbulent transport term Tr_{mf} was also previously recognised by Folk et al. [25,26] who used rapid distortion theory to estimate the magnitude of this term for turbine flow exposed to combustor turbulence. As far as Tr_{ff} term is concerned, it appears to be entirely determined by the streamwise fluctuations u' and turbulent kinetic energy $\frac{1}{2}u'_i u'_i$.

CONCLUSIONS

A series of high fidelity datasets of compressor cascades at varying inflow conditions was analysed in this paper. For each of the cases a comparison between entropy, enthalpy and stagnation pressure loss coefficient was carried out. To understand the difference between the entropy loss coefficient and stagnation pressure loss coefficient a transport equation budget was performed for both terms. This resulted in the following list of conclusions.

While entropy and enthalpy gave almost identical loss predictions, stagnation pressure loss coefficient was found to be unreliable loss metric for cases considered here under-predicting loss for one of the cases by as much as 40% when compared to the entropy loss coefficient (*NACA65 Gap30* case). This was the case despite all the simulations were run at adiabatic and low Mach number conditions. The use of stagnation pressure estimate discarding turbulent kinetic energy resulted in even more unreliable predictions highlighting the importance of including it when comparing experimental data with RANS for highly unsteady flowfields.

To understand the discrepancy between loss coefficients, entropy and stagnation pressure transport equation budgets were performed. All the budgets were fully balanced and allowed to elucidate the origin of the discrepancy. This was traced to the turbulent transport terms which arise as part of the stagnation pressure transport equation. These terms were found to be primarily present in the freestream. A commonly used assumption of its negligible contribution to the overall budget was found to be wrong even when only moderate levels of inflow turbulence were present. The combined impact of these terms was found to be negative for a compressor resulting in artificially lower loss estimates by the stagnation pressure loss coefficient. This was linked to flow deceleration in a compressor. For a turbine flow, loss estimates are likely to be artificially higher due to the flow

acceleration.

The use of stagnation pressure loss coefficient may still be valid when low levels of inflow unsteadiness are present and when turbulent transport is low. The impact also appears to be more pronounced for the cases at lower Reynolds number. In addition it was shown that integrated turbulent transport terms were low within the boundary layers and wake. As a result loss predicted by entropy and stagnation pressure in those regions was in good agreement. In experimental setting, however, such decomposition may be difficult to achieve, while estimating turbulent transport is beyond current standard experimental practice.

ACKNOWLEDGMENT

The authors would also like to acknowledge the help of UK Turbulence Consortium funded by the EPSRC grant *EP/L000261/1* and Cambridge Service for Data Driven Discovery system operated by the University of Cambridge Research Computing Service funded by EPSRC Tier-2 grant *EP/P020259/1*, whose HPC allocations have been used to obtain the results. This project has received funding from the European Union's Horizon 2020 research and innovation programme under the Marie Skłodowska-Curie grant agreement No [101026928] and this support is also gratefully acknowledged. We also acknowledge PRACE, which awarded access to the Fenix Infrastructure resources at CINECA, partially funded from the European Union's Horizon 2020 research and innovation program through the ICEI project under the grant agreement No.800858.

REFERENCES

- [1] Sandberg, R. D., and Michelassi, V., 2022. "Fluid dynamics of axial turbomachinery: Blade-and stage-level simulations and models". *Annual Review of Fluid Mechanics*, **54**, pp. 255–285.
- [2] Denton, J. D., 1993. "Loss mechanisms in turbomachines". *ASME. J. Turbomach. October 1993; 115(4): 621–656*.
- [3] Miller, R. J., 2013. "Mechanical work potential". In *Turbo Expo: Power for Land, Sea, and Air*, ASME paper no. GT2013-95488, American Society of Mechanical Engineers.
- [4] Moore, J., Shaffer, D., and Moore, J., 1987. "Reynolds stresses and dissipation mechanisms downstream of a turbine cascade". *ASME J. Turbomach. April 1987; 109:258–267*.
- [5] Tennekes, H., and Lumley, J., 1972. *A first course in turbulence*. MIT press.
- [6] Stieger, R. D., and Hodson, H. P., 2005. "The unsteady development of a turbulent wake through a downstream low-pressure turbine blade passage.". *ASME. J. Turbomach. 2005; 127(2):388-394*.

TABLE 7: Contribution of different components to turbulent transport Tr_{mf}

	NACA65		NACA65			CDA		
	Tu4	Tu6	Gap30	Gap40	Gap50	Gap30	Gap40	Gap50
$\frac{\partial}{\partial x} [\bar{u} (\overline{\rho u' u'})] / Tr_{mf}$	0.74	0.85	1.09	1.14	1.13	2.45	3.82	3.64
$\frac{\partial}{\partial x} [\bar{v} (\overline{\rho u' v'})] / Tr_{mf}$	0.26	0.15	-0.09	-0.14	-0.14	-1.44	-2.79	-2.61
$\frac{\partial}{\partial x} \left[\overline{\rho u' \left(\frac{1}{2} u' u' \right)} \right] / Tr_{ff}$	-	-	0.87	0.87	0.86	0.67	0.74	0.74
$\frac{\partial}{\partial x} \left[\overline{\rho u' \left(\frac{1}{2} v' v' \right)} \right] / Tr_{ff}$	-	-	0.07	0.07	0.07	0.25	0.22	0.21
$\frac{\partial}{\partial x} \left[\overline{\rho u' \left(\frac{1}{2} w' w' \right)} \right] / Tr_{ff}$	-	-	0.06	0.06	0.07	0.08	0.05	0.04

- [7] MacIsaac, G., Sjolander, S., and Praisner, T., 2012. "Measurements of losses and reynolds stresses in the secondary flow downstream of a low-speed linear turbine cascade". *ASME J. Turbomach. November 2012; 134:061015-1-12*.
- [8] Lengani, D., Simoni, D., Ubaldi, M., Zunino, P., Bertini, F., and Michelassi, V., 2017. "Accurate estimation of profile losses and analysis of loss generation mechanisms in a turbine cascade". *Journal of Turbomachinery*, **139**(12), p. 121007.
- [9] Wu, X., and Durbin, P. A., 2001. "Evidence of longitudinal vortices evolved from distorted wakes in a turbine passage". *J. Fluid Mech.*, **446**, pp. 199–228.
- [10] Michelassi, V., and Wissink, J. G., 2015. "Turbulent kinetic energy production in the vane of a low-pressure linear cascade with incoming wakes". *International J. of Rotating Machinery, Vol. 2015*.
- [11] Wheeler, A. P., Sandberg, R. D., Sandham, N. D., Pichler, R., Michelassi, V., and Laskowski, G., 2016. "Direct numerical simulations of a high-pressure turbine vane". *Journal of Turbomachinery*, **138**(7).
- [12] Przytarski, P. J., and Wheeler, A. P., 2020. "The effect of gapping on compressor performance". *Journal of Turbomachinery*, **142**(12).
- [13] Leggett, J., Richardson, E., Priebe, S., Shabbir, A., Michelassi, V., and Sandberg, R., 2020. "Loss analysis of unsteady turbomachinery flows based on the mechanical work potential". *Journal of Turbomachinery*, **142**(11).
- [14] Przytarski, P. J., and Wheeler, A. P., 2021. "Accurate prediction of loss using high fidelity methods". *Journal of Turbomachinery*, **143**(3).
- [15] Leggett, J., Zhao, Y., Richardson, E. S., and Sandberg, R. D., 2021. "Turbomachinery loss analysis: the relationship between mechanical work potential and entropy analyses". In Turbo Expo: Power for Land, Sea, and Air, ASME paper no. GT2021-59436, American Society of Mechanical Engineers.
- [16] Miki, K., and Ameri, A., 2022. "Numerical investigation of the effect of trailing edge thickness of simulated cmc blades on loss profiles". In Turbo Expo: Power for Land, Sea, and Air, ASME paper no. GT2022-82335, American Society of Mechanical Engineers.
- [17] Wheeler, A. P. S., Dickens, A. M. J., and Miller, R. J., 2018. "The effect of non-equilibrium boundary layers on compressor performance". *Journal of Turbomachinery*.
- [18] Brown, L. E., 1972. "Axial flow compressor and turbine loss coefficients: A comparison of several parameters". *ASME Conference Proceedings, no. 72-GT-18*.
- [19] Jardine, L., 2019. "The effect of heat transfer on turbine performance". *Doctoral thesis, University of Cambridge*.
- [20] Cantwell, B., 2013. *AA200: Applied Aerodynamics*. Stanford University.
- [21] Zhao, Y., and Sandberg, R. D., 2020. "Using a new entropy loss analysis to assess the accuracy of rans predictions of an high-pressure turbine vane". *Journal of Turbomachinery*.
- [22] Hinze, J. O., 1975. *Turbulence*. New York McGraw Hill.
- [23] Perdichizzi, A., Ubaldi, M., and Zunino, P., 1990. "A hot wire measuring technique for mean velocity and reynolds stress components in compressible flow". In Measuring Techniques in Turbomachinery, MTT1090, American Society of Mechanical Engineers.
- [24] Jelly, T. O., Day, I. J., and di Mare, L., 2017. "Phase-averaged flow statistics in compressors using a rotated hot-wire technique". *Exp. Fluids*.
- [25] Folk, M., 2019. "The impact of combustor turbulence on loss mechanisms in the high pressure turbine". *Doctoral thesis, University of Cambridge*.

- [26] Folk, M., Miller, R. J., and Coull, J. D., 2020. “The impact of combustor turbulence on turbine loss mechanisms”. *Journal of Turbomachinery*.
- [27] Aupoix, B., Blaisdell, G. A., Reynolds, C. W., and Zeman, O., 1990. “Modelling the turbulent kinetic energy equations for compressible, homogeneous turbulence”. In *Proceedings of the Summer Program 1990, N92-30653*, Center for Turbulence Research.

Appendix A: Double decomposition of kinetic energy

Considerable insight can be drawn from the analysis of kinetic energy budget. Using Reynolds decomposition kinetic energy can be decomposed into mean (m) and fluctuating (f) components (full derivation available e.g. at [27]):

$$\begin{aligned}
 \underbrace{\frac{\bar{D}}{Dt} \left(\bar{\rho} \frac{1}{2} \bar{u}_i \bar{u}_i \right)}_{adv_m} &= - \underbrace{\bar{u}_i \frac{\partial \bar{p}}{\partial x_i}}_{pw_m} \\
 &- \underbrace{\left(-\overline{\rho u'_i u'_j} \frac{\partial \bar{u}_i}{\partial x_j} \right)}_{t_{mf}} - \underbrace{\frac{\partial}{\partial x_j} \left[\bar{u}_i \left(\overline{\rho u'_i u'_j} \right) \right]}_{tr_{mf}} \\
 &+ \underbrace{\frac{\partial \bar{\tau}_{ij} \bar{u}_i}{\partial x_j}}_{vd_m} - \underbrace{\bar{\tau}_{ij} \frac{\partial \bar{u}_i}{\partial x_j}}_{\phi_m}
 \end{aligned} \tag{20a}$$

$$\begin{aligned}
 \underbrace{\frac{\bar{D}}{Dt} \left(\bar{\rho} \frac{1}{2} \overline{u'_i u'_i} \right)}_{adv_f} &= \\
 &+ \underbrace{\left(-\overline{\rho u'_i u'_j} \frac{\partial \bar{u}_i}{\partial x_j} \right)}_{t_{mf}} - \underbrace{\frac{\partial}{\partial x_j} \left[\overline{\rho u'_j} \left(\frac{1}{2} \overline{u'_i u'_i} \right) \right]}_{tr_{ff}} \\
 &+ \underbrace{\frac{\partial \overline{\tau'_{ij} u'_i}}{\partial x_j}}_{vd_f} - \underbrace{\overline{\tau'_{ij}} \frac{\partial \overline{u'_i}}{\partial x_j}}_{\phi_f} - \underbrace{\overline{u'_i} \frac{\partial \bar{p}}{\partial x_i}}_{pw_f} - \underbrace{\frac{\partial \overline{p' u'_i}}{\partial x_i}}_{pd_f} + \underbrace{\overline{p' \frac{\partial u'_i}{\partial x_i}}}_{pl_f}
 \end{aligned} \tag{20b}$$

where

$$\frac{\bar{D}}{Dt} \equiv \frac{\partial}{\partial t} + \bar{u}_j \frac{\partial}{\partial x_j} \tag{21}$$

and

adv - convection of kinetic energy
pw - pressure work

t - energy transfer between mean and fluctuating flowfield (turbulence production)
tr - diffusion due to unsteadiness/turbulence
vd - viscous diffusion
 ϕ - viscous dissipation
pd - pressure diffusion
pl - pressure dilation

Table A1 shows that mean kinetic energy budgets is satisfied. For turbulent kinetic energy budget the balance was achieved when artificial dissipation was added to the resolved dissipation, Table A2. This further validates the methodology taken in this study.

TABLE A1: Double decomposition - mean kinetic energy budget

$$Adv_m = -PW_m + \mathcal{T}_{mf} - Tr_{mf} + VD_m - \Phi_m$$

	NACA65		NACA65			CDA		
	Tu4	Tu6	Gap30	Gap40	Gap50	Gap30	Gap40	Gap50
Adv_m	111.1445	110.9216	107.7270	109.5839	109.9521	46763.7137	46822.3687	46945.5559
PW_m	-105.2509	-106.1870	-105.9626	-106.2991	-105.8217	-45480.7915	-45432.2649	-45490.2992
\mathcal{T}_{mf}	3.1712	3.3751	2.3372	2.4060	2.5776	695.0648	750.2811	780.8226
Tr_{mf}	0.8466	2.5871	3.9051	2.5509	2.0044	387.6402	207.1210	208.5881
VD_m	0.0118	0.0090	0.0139	0.0145	0.0147	2.4507	2.2288	2.2402
Φ_m	3.5879	3.6597	3.4189	3.4715	3.5539	962.0147	904.6694	911.7720
LHS - RHS	-0.0070	0.2958	-0.0727	-0.0273	0.0179	15.9336	-55.4968	-26.5095

TABLE A2: Double decomposition - turbulent kinetic energy budget

$$Adv_f = -PW_f + \mathcal{T}_{mf} - Tr_{ff} + VD_f - \Phi_f - PD_f + PL_f$$

	NACA65		NACA65			CDA		
	Tu4	Tu6	Gap30	Gap40	Gap50	Gap30	Gap40	Gap50
Adv_f	0.7976	2.8418	2.0468	1.5165	1.1772	533.4470	501.4282	474.7137
PW_f	-	-	-	-	-	-	-	-
\mathcal{T}_{mf}	3.1712	3.3751	2.3372	2.4060	2.5776	695.0648	750.2811	780.8226
Tr_{ff}	0.0000	0.0000	-0.6882	-0.6488	-0.4883	-94.2817	-213.8627	-202.5755
VD_f	0.0083	0.0167	0.0052	0.0050	0.0051	1.8809	1.5766	1.5437
Φ_{f+N}	3.9764	6.2947	3.5608	3.1964	3.1722	1149.2538	1011.4609	1004.9839
PD_f	-	-	-0.1294	-0.0801	-0.1112	-4.8095	-26.3358	-33.4561
PL_f	-	-	-	-	-	-	-	-
LHS - RHS	0.0007	-0.0610	0.0108	0.0021	-0.0118	-17.9523	1.6265	16.0645